Polymeric Coordination Complexes Based on Cobalt, Nickel, and Ruthenium That Exhibit Synergistic Thermal Properties

Laurence A. Belfiore,* Mary Pat McCurdie, and Eiji Ueda†

Polymer Physics and Engineering Laboratory, Department of Chemical Engineering, Colorado State University, Fort Collins, Colorado 80523

Received April 19, 1993; Revised Manuscript Received August 30, 1993®

ABSTRACT: d-Block transition-metal-containing polymer blends which form coordination complexes are the focus of this research. The model compounds are cobalt chloride hexahydrate, nickel acetate tetrahydrate, and the dimer of dichlorotricarbonylruthenium(II). The ligand is poly(4-vinylpyridine), P4VP, or copolymers that contain 4-vinylpyridine repeat units. Thermal analysis via differential scanning calorimetry suggests that the glass transition temperature of the polymeric ligand(s) is enhanced by these d-block metal salts in binary and ternary blends. Cobalt and nickel salts function as transition-metal compatibilizers for two immiscible copolymers of styrene with 4-vinylpyridine and butyl methacrylate with 4-vinylpyridine. At the molecular level, Fourier transform infrared spectroscopy of P4VP–ruthenium precipitates reveals that the pyridine nitrogen lone pair coordinates to the metal center and strengthens ruthenium–carbonyl bonds in the polymeric complex. Infrared absorption frequencies of the CO ligands are consistent with π-backbonding between the t_{2g} molecular orbitals of the metal in the octahedral point group and the π^* antibonding orbitals of carbon monoxide. High-resolution carbon-13 solid-state NMR spectroscopy identifies at least two, and possibly three, carbonyl signals in the undiluted pseudooctahedral ruthenium dimer via the Bloch-decay pulse sequence. In the polymeric complex, carbonyl ^{13}C magnetization unique to the ruthenium salt is generated via intermolecular polarization transfer from the proton spin manifold of poly(4-vinylpyridine) using a cross-polarization thermal mixing time of 2 ms. Since there are no protons in the ruthenium dimer, the observation of energy-conserving ^1H–^{13}C spin diffusion between dissimilar molecules under matched Hartmann–Hahn spin-lock conditions argues convincingly that heteronuclear dipolar distances are small enough for the proposed polymeric complex to form. A thermodynamic interpretation of ligand field stabilization energies appropriate to tetrahedral cobalt complexes is employed to estimate the synergistic enhancement of the glass transition temperature, particularly when coordination cross-links are present.

Transition-metal coordination in polymer blends represents an important mechanism to induce compatibility between dissimilar components and generate systems that exhibit superior macroscopic physical properties relative to the undiluted raw materials. The key component in these blends is a low-molecular-weight salt that contains a metal center with incompletely filled d-electronic orbitals. Materials of this nature are of interest because it has been demonstrated that energetic stabilization due to the ligand field can enhance thermochemical and mechanicochemical properties of the polymeric ligand.[1–5] One advantage of employing low-molecular-weight d-block transition metal salts is that coordination and symmetry in the undiluted crystalline state is known prior to blending via X-ray diffraction data.[6–10] In this respect, cobalt chloride hexahydrate,[6,7] nickel acetate tetrahydrate,[8,9] and the dimer of dichlorotricarbonylruthenium(II)[10] are blended with amorphous polymers and copolymers that contain 4-vinylpyridine repeat units in the main chain. The lone pair on nitrogen represents a strongly basic ligand that is known to coordinate to transition metals.[11–15] Strong interactions in polymer blends via hydrogen bonding have been the subject of numerous scientific investigations for more than three decades, now. Hence, it is reasonable to search for systems that exhibit stronger interaction via different blending mechanisms. d-Block metal centers with multiple ligands in their coordination sphere represent one of the focal points for future studies of strong interaction and compatibilization in polymer blends. This novel concept is pursued from a macroscopic and molecular engineering viewpoint. Enhancement of the glass transition temperature is interpreted as a manifestation of the fact that the disruption of "coordination cross-links" is an endothermic process.[2]

Nickel Complexes. Previous research in our laboratory identified blends of nickel acetate tetrahydrate with poly(4-vinylpyridine) that exhibit synergistic thermal response in the glass transition temperature phase diagram.[1,2,5] This is a consequence of coordination cross-links where, in the most favorable situation, the pseudooctahedral nickel cation forms metal–ligand bonds with pyridine pendant groups on two different macromolecular chains. Six-coordinate d^8 nickel complexes are strongly favored from an equilibrium viewpoint when good donor ligands such as pyridine are present.[16] The work described herein employs nickel acetate tetrahydrate as a transition metal compatibilizer for two immiscible copolymers of 4-vinylpyridine with styrene, and 4-vinylpyridine with butyl methacrylate. Both copolymers are soluble in formic acid, and nickel acetate is dissolved in acetic acid. Precipitation does not occur when all of the components are mixed. The five-component liquid mixture and the solid ternary residue after solvent evaporation exhibit a greenish color. A simplistic molecular model that exploits the octahedral bonding characteristics of nickel is used to postulate the microstructure of the green transparent ternary blends that have glass transition temperatures in excess of 200 °C.

Cobalt Complexes. Cobalt chloride hexahydrate is used to generate transition-metal complexes with polymeric pyridine ligands. Two independent X-ray crystallographic studies have deduced a pseudooctahedral geometry for $CoCl_2(H_2O)_6$ with two chloride anions and four waters of hydration coordinated to the metal center.[6,7] The two remaining waters of hydration are "free", but they reside near the chlorides and form hydrogen bonds with these anions. The hexahydrate is pink and the

* Author to whom correspondence should be addressed.
† Permanent address: Asahi Chemical Industry, Okayama Prefecture, Japan.
® Abstract published in *Advance ACS Abstracts*, October 15, 1993.

0024-9297/93/2226-6908$04.00/0

Table I. Details of the Blend Preparation Sequence

polymer	d-block salt	mol % salt	solvent	precipitate/color	molding temp (°C)
P4VP	$CoCl_2$	5	ethanol	yes/blue	200
		10	ethanol	yes/blue	230
		20	ethanol	yes/blue	unsuccessful at 300 °C
4VP/S, 4VP/BMA	$CoCl_2$	5	formic acid	no	170
		11	formic acid	no	190
4VP/S, 4VP/BMA	$Ni[OOCCH_3]_2$	all blends	acetic acid / formic acid	no	none
P4VP	$Ru(CO)_3Cl_2$ dimer	1–10	CH_2Cl_2	no	none
		50	CH_2Cl_2 w/N_2 purge	yes/yellow-brown	unsuccessful at 300 °C

anhydrous salt is blue.[6] X-ray diffraction data on dark blue crystals of dichlorobis(4-vinylpyridine)cobalt(II) suggest that the structure of this four-coordinate pseudotetrahedral complex contains two 4-vinylpyridine ligands and no waters of hydration.[17–19] These studies are significant because they demonstrate that the borderline acid Co^{2+} sheds its four hard-base waters of hydration in favor of two pyridine ligands which are classified as a borderline base.[20] Tetrahedral symmetry of the metal center is a common occurrance for d^7 Co^{2+} complexes.[21] Cobalt complexes with poly(4-vinylpyridine) were prepared from ethanol solution, generating blue precipitates. Ternary blends of cobalt chloride with the same two immiscible 4-vinylpyridine copoloymers mentioned above were prepared in formic acid to generate pink solutions without precipitate formation. These pink solutions produced blue solid complexes after solvent evaporation at ambient temperature followed by vacuum drying at 100 °C for more than 24 h.

Ruthenium Complexes. Ruthenium carbonyl complexes are of interest because carbonyl ligands contribute favorably to strong-field zero-spin (i.e., diamagnetic) behavior for a d^6 metal center with pseudooctahedral symmetry.[21] Under these conditions, the ligand field stabilization energy is 240% of the ligand field splitting. Octahedral ligand field splittings increase (i) as one moves down a group in the periodic table toward the heavier metals like ruthenium, which is found in the second row of the d-block, (ii) when stronger σ-donor ligands like pyridine coordinate to the metal center, and (iii) when backbonding to π-acceptor ligands like CO lowers the energy of the t_{2g} metal-based molecular orbitals. The divalent ruthenium cation is classified as a borderline acid[20] which exhibits an affinity for borderline bases like the polymeric pyridine ligands employed in this study. Consequently, octahedral ruthenium(II) complexes should exhibit large increases in the glass transition temperature relative to the T_g of undiluted poly(4-vinylpyridine). Reactions of $[Ru(CO)_3Cl_2]_2$ with both stoichiometric and excess amounts of pyridine are well documented.[22,23] In both cases, the dihalogen bridge is cleaved and either one or two pyridine ligands coordinate to each metal center forming complexes with pseudooctahedral symmetry. The second pyridine ligand displaces carbon monoxide in the coordination sphere of the metal. Vibrational spectroscopic studies of $[Ru(CO)_3Cl_2]_2$ in the vicinity of 1900–2200 cm^{-1} fingerprint the infrared absorptions of CO which are sensitive to the σ- and π-bonding characteristics of the ligands.[22,24] It is well-known that electron-rich metal centers can backbond to π-acceptor ligands like CO and shift the vibrational absorption frequencies of carbon monoxide to lower energy.[21] Infrared data for CO illustrated herein suggest that pyridine ligands in the side group of poly(4-vinylpyridine) cleave the dihalogen bridge of the low-molecular-weight ruthenium salt when polymeric complexes form. Solid-state carbon-13 NMR spectroscopic data reveal that heteronuclear spin diffusion between protons in P4VP and the carbonyl carbons of the ruthenium salt is operative. This observation of intermolecular polarization transfer is consistent with micromixing of two dissimilar blend components. Poly(4-vinylpyridine) and $[Ru(CO)_3Cl_2]_2$ were dissolved separately in methylene chloride at 25 °C under a nitrogen atmosphere. A yellowish brown powdery precipitate forms when the two solutions are mixed. The stoichiometric blend which contains an approximate 1:1 molar ratio of ruthenium to pyridine nitrogen exhibits a glass transition temperature in excess of 300 °C.

Experimental Section

Materials. Cobalt chloride hexahydrate, nickel acetate tetrahydrate, and the dimer of dichlorotricarbonylruthenium-(II) were purchased from Aldrich Chemical Co. in Milwaukee, WI. Poly(4-vinylpyridine), MW = 200 kDa, and the two copolymers that contain 4-vinylpyridine repeat units were obtained from Scientific Polymer Products in Ontario, NY. Styrene/4-vinylpyridine (4VP/S) and butyl methacrylate/4-vinylpyridine (4VP/BMA) both contain 50 wt % of each comonomer. This corresponds to a 50/50 molar ratio of styrene and 4-vinylpyridine in the 4VP/S copolymer and a 58/42 molar ratio of 4-vinylpyridine to butyl methacrylate in the 4VP/BMA copolymer. All materials were blended as received from the commercial distributors without further purification. The solvents used were reagent grade.

Sample Preparation Methods. 4-Vinylpyridine polymers or copolymers were blended with low-molecular-weight d-block transition metal salts via dilute solution procedures at ambient temperature. The total solids content in each case was approximately 2% (w/v). Solvent evaporation was accomplished via air-drying at ambient temperature in a fume hood for 24–72 h. When precipitation occurred, both the precipitate and the supernatant were dried together to recover all of the solid material that was initially dissolved in the solvent. In this fashion, the composition of each blend was determined from the weights of the starting materials before dissolution. Solid residues were subsequently dried under vacuum for 24–48 h at the following temperatures: (i) 100 °C for cobalt and nickel complexes, and (ii) 60 °C for the ruthenium complex. Color changes were observed only for the ternary residues of cobalt chloride with both copolymers after vacuum drying. In some cases, the vacuum-dried residues were compression molded using a Carver press at the temperatures indicated in Table I. Compression molding facilitates homogenization when precipitates form because the solvent evaporation step deposits a solid residue from the supernatant onto the precipitate and on the bottom of the Petrie dish. Molding is not feasible when the glass transition temperature is enhanced significantly because excessive temperatures are required that can easily induce thermal decomposition of the d-block transition metal salt as well as the polymer. On the other hand, oxidation–reduction potentials suggest that it is highly unlikely for these particular divalent metal cations to oxidize the ligands and modify the structure of the polymeric complex.

Differential Scanning Calorimetry. Thermal analysis was performed on a Perkin-Elmer DSC-7 with the overall goal of generating temperature-composition phase diagrams. After quenching from the molten state, glass transition temperatures were measured at a rate of 20 °C/min during the second or third heating trace *in the calorimeter* under helium and nitrogen purges. T_g was calculated at the midpoint of the heat capacity change between the liquid and glassy states, without complicating

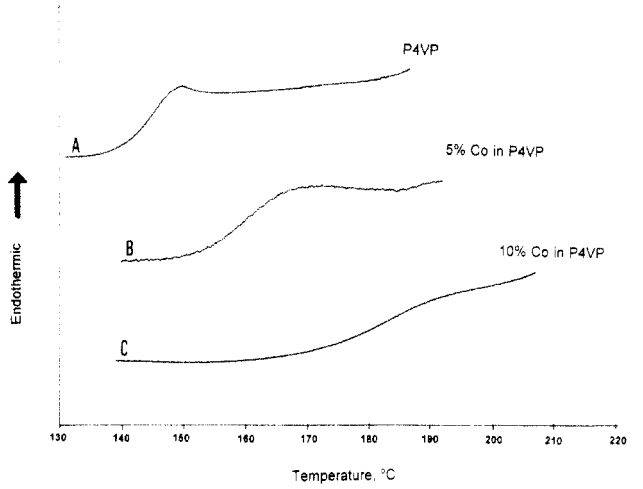

Figure 1. Differential scanning calorimetry thermograms for coordination complexes of poly(4-vinylpyridine) and cobalt chloride. The uppermost trace (A) represents the undiluted polymer, and the molar concentration of the metal salt is provided at the right of the lower two traces (B, C).

effects due to enthalpy relaxation. Differential power output was monitored via Perkin-Elmer's TAC 7/DX thermal analysis controller in conjunction with the DSC7 multitasking software on a 386/33 home-built personal computer.

Carbon-13 Solid-State NMR Spectroscopy. Proton-enhanced dipolar-decoupled carbon-13 solid-state NMR spectra were obtained on a Chemagnetics CMX 300-MHz spectrometer in collaboration with Dr. James S. Frye at Otsuka Electronics Inc., Fort Collins, CO. The carbon frequency was 75.479 MHz and magic-angle spinning (MAS) was performed at frequencies between 4000 and 6500 Hz. The spectrometer incorporates a 7.5-mm Coax probe. A proton 90° pulse width of 4 μs was employed, corresponding to an rf field strength of 62.5 kHz. The rf field was maintained at 62.5 kHz during cross polarization (CP) and subsequent high-power ^{1}H decoupling. The ^{1}H–^{13}C cross polarization contact time was 2 ms, and the pulse repetition delay was 2 s. Since proton spin-lattice relaxation times for poly(4-vinylpyridine) in the laboratory frame are less than 1 s, the ^{13}C CP/MAS NMR spectra are fully relaxed and contain information about all regions of the sample that respond to a contact time of 2 ms. Single-pulse Bloch decay spectra were acquired for the undiluted ruthenium dimer and the polymeric ruthenium complex using pulse repetition delays of 60 and 30 s, respectively. Carbon-13 free induction decays (FIDs) were accumulated via 1024 time-domain data points. Prior to Fourier transformation, the signal-averaged FID was zero-filled to 8K. The spectral width encompassed a 40-kHz frequency range and 50 Hz of line broadening was employed. Carbon-13 chemical shifts were referenced externally to the methyl resonance of hexamethylbenzene, 17.355 ppm deshielded from tetramethylsilane (TMS).

Fourier Transform Infrared Spectroscopy. FTIR measurements of the P4VP/ruthenium precipitate and undiluted $[Ru(CO)_3Cl_2]_2$ were obtained from powders in a KBr medium at ambient temperature. The infrared spectrum of undiluted poly(4-vinylpyridine) was obtained as a thin glassy film cast from solution onto a KBr crystal. A Galaxy series Model 5020 FTIR from Mattson Instruments was employed to perform the desired task. The optical bench is interfaced to a 486/50-MHz personal computer for data acquisition and control. Each spectrum was generated by signal averaging 64 scans at a resolution of either 1.0 or 2.0 cm^{-1}, and a triangular apodization smoothing function was employed.

Results and Discussion

Cobalt Complexes with Poly(4-vinylpyridine). Binary mixtures of cobalt chloride with P4VP exhibit glass transition temperatures of 160 °C and 183 °C when the molar concentration of the metal salt is 5 and 10%, respectively. These results are illustrated via calorimetry traces in Figure 1. For comparison, the measured T_g of undiluted poly(4-vinylpyridine) is 145 °C. No glass transition is detected by differential scanning calorimetry for a sample containing 20 mol % cobalt chloride that was heated to 250 °C. This observation is consistent with the fact that the 20 mol % blend could not be compression molded at 300 °C. Tetrahedral coordination of the metal center to two chloride anions and two pyridine side groups in P4VP is consistent with (i) the color of the polymeric complex[18,19] and (ii) previously reported results based on dichlorobis(4-vinylpyridine)cobalt(II).[17] Cross-link formation via metal–ligand interaction is not unique to solid complexes that contain cobalt, nickel, or ruthenium as described herein. Shibayama et al.[38] observed gelation in aqueous solutions of poly(vinyl alcohol) with a specific class of vanadate ions that are thermodynamically favored over a restricted range of vanadate concentrations and pH. Both intra- and intermolecular cross-links have been proposed via hydrogen bonds between the OH side group in the polymer and the apical oxygens of the $[V_{10}O_{28}]^{6-}$ cagelike structure.[38] These cross-link models provide a reasonable explanation of solution viscosity data above and below the critical polymer concentration for overlap or entanglement formation.

The synergistic increase in the glass transition temperature for blends of P4VP and cobalt chloride is described from an energetic viewpoint by focusing on the electronic energy of the metal d-electrons and the subsequent ligand field stabilization for complexes with pseudotetrahedral symmetry. Even though ligand field stabilization energies represent only a small fraction of metal–ligand bond energies, the empirical correlation with glass transition temperature enhancement is very encouraging. The absolute magnitude of T_g and the discontinuous observable ΔC_p at the glass transition are not predicted by the energetic ligand field stabilization model. Quantum mechanical group contribution methods are applicable to estimate the octahedral ligand field splitting of various mono-ligand six-coordinate complexes.[25] The analogous four-coordinate complexes with tetrahedral symmetry exhibit ligand field splittings that are 4/9th as large as the corresponding octahedral values.[21,25] In this respect, the following tetrahedral ligand field splittings are calculated: Δ_T = 3289 cm^{-1} for the four-coordinate cobalt chloride anion $[CoCl_4]^{2-}$, Δ_T = 4133 cm^{-1} for the tetraaqua cation $[Co(H_2O)_4]^{2+}$, and Δ_T = 5167 cm^{-1} for the four-coordinate cobalt pyridine cation $[Co(C_5H_5N)_4]^{2+}$. The "rule of average environments" is subsequently invoked which states that "*the ligand field splitting for a pseudotetrahedral mixed-ligand complex is a weighted average of the splittings calculated for each of the mono-ligand four-coordinate complexes separately*". Hence, one estimates the pseudotetrahedral ligand field splitting Δ_T for two mixed-ligand complexes which represent models of (i) a blue polymeric cobalt complex where the metal center coordinates to pyridine side groups on two different macromolecular chains, and (ii) the complex that survives after enough thermal energy is supplied to remove one pyridine ligand from the coordination sphere of the metal center and induce the glass transition. The first blue complex is $CoCl_2(C_5H_5N)_2$, illustrated in Figure 2a, with an estimated ligand field splitting of Δ_T = 4228 cm^{-1}. After dissociation of the coordination cross-links, the latter blue complex is $CoCl_2(C_5H_5N)(H_2O)$ with Δ_T = 3969 cm^{-1} as illustrated in Figure 2b. The ligand field stabilization energy for each model complex is based on the energy difference between the frontier molecular orbitals of the metal and the electronic configuration for a d^7 complex.

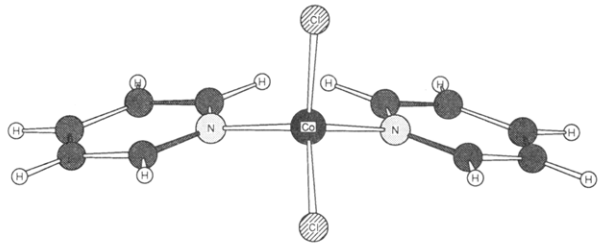

(a) LFSE = 60.7 KJ/mole

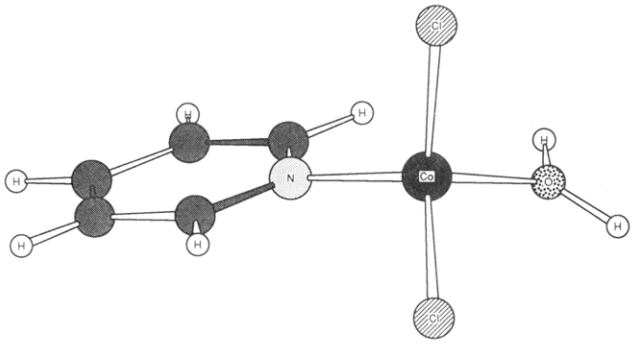

(b) LFSE = 57.0 KJ/mole

Figure 2. Simple tetrahedral molecular models of coordination complexes between cobalt chloride and pyridine side groups in P4VP illustrating (a) coordination cross-links that are responsible for enhanced glass transition temperatures, and (b) the complex that survives after thermal energy is supplied to induce cross-link dissociation via removal of one pyridine side group from the coordination sphere of the metal center. In each case, the ligand field stabilization energy (LFSE) is estimated from empirical "group-contribution" methods.

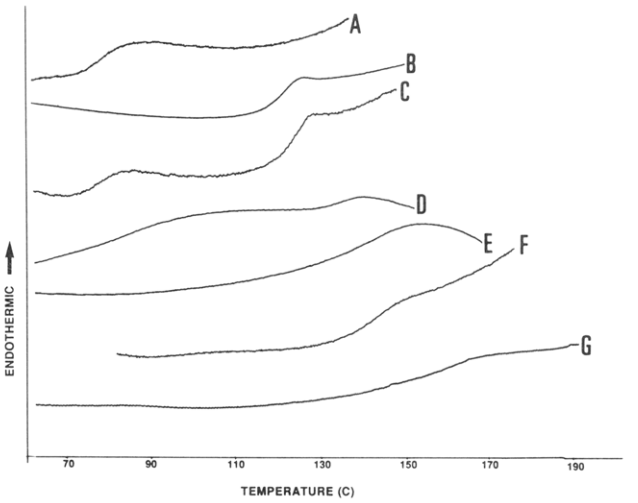

Figure 3. Differential scanning calorimetry thermograms for compatibilized ternary blends that contain either cobalt chloride or nickel acetate with two immiscible 4-vinylpyridine copolymers. The two uppermost traces represent the temperature dependence of the specific heat for undiluted copolymers of (A) butyl methacrylate with 4-vinylpyridine (4VP/BMA) and (B) styrene with 4-vinylpyridine (4VP/S). Thermogram C illustrates classic incompatibility of a 50/50 mixture of these two copolymers on a weight fraction basis. Thermograms D and E are representative of ternary blends of these two copolymers with 3 and 9 mol % nickel acetate tetrahydrate, respectively. Thermograms F and G correspond to ternary blends of the same two copolymers with 5 and 11 mol % cobalt chloride hexahydrate, respectively. The ternary blends contain a 55/45 molar ratio of 4VP/S and 4VP/BMA, as well as the above-mentioned concentrations of the metal salt.

For tetrahedral symmetry, the five degenerate d-atomic orbitals of the free metal ion split into a set of two molecular orbitals (designated e) that are 60% lower in energy and a triply degenerate set (t_2) that are 40% higher in energy.[21] For an electronic configuration of $e^4(t_2)^3$, which is independent of the strength of the ligand field, the ligand field stabilization energy (LFSE) is 120% of the energy difference between the e and t_2 molecular orbitals. This energy difference between frontier orbitals is calculated above as the ligand field splitting, Δ_T. Hence, the LFSE of $CoCl_2(C_5H_5N)_2$ is 3.7 kJ/mol greater than the LFSE of $CoCl_2(C_5H_5N)(H_2O)$ as indicated in Figure 2. This is reasonable because pyridine is a stronger base than the water of hydration.[21,26] Furthermore, the former complex represents a model of coordination cross-links where the mobility of the polymer chains is severely restricted. Thermal energy must be supplied to dissociate coordination cross-links and arrive at the latter model complex where the energy of the metal d-electrons is higher based on LFSE calculations. The synergistic increase in T_g is modeled as follows: $R\Delta T_g = (\Delta\text{LFSE})\beta x(1-x)$, where the left-hand side represents thermal energy that must be supplied to induce the glass transition of the polymeric cobalt complex relative to the undiluted polymer, and the right-hand side represents the energy difference between metal d-electrons for a coordination cross-link vs a coordination pendant group. Concentration dependence of the coordination interaction is assumed to follow the Margules model for nonideal energetics where x represents the mole fraction of the metal salt. A parameter β, which is realistically less than unity, has been included on the right-hand side of the above equation because predictions of bonding in low-molecular-weight crystalline coordination complexes overestimate experimental measurements for amorphous polymeric materials. The "best fit" value of β is 0.82 for transition-metal complexes that contain 5 and 10 mol % cobalt chloride. A previous treatment of ligand field stabilization to describe thermal synergy in pseudooctahedral complexes of nickel acetate with P4VP generated values of β in the 70% range and Δ(LFSE) = 5.3 kJ/mol.[2]

Cobalt and Nickel Complexes with Two Immiscible 4-Vinylpyridine Copolymers. An interesting application of the methodology discussed above employs low-molecular-weight d-block metal salts to form coordination cross-links with pyridine side groups on two immiscible 4-vinylpyridine copolymers. Both nickel acetate and cobalt chloride are transition-metal compatibilizers for random copolymers of styrene with 4-vinylpyridine (4VP/S), and butyl methacrylate with 4-vinylpyridine (4VP/BMA). Jiang et al.[40] have *partially compatibilized* the same two types of copolymers via divalent d-block metal salts based on cobalt, magnesium, copper, and zinc. The 58/42 copolymer of 4-vinylpyridine and butyl methacrylate exhibits a glass transition temperature of 80 °C (Figure 3A), whereas the T_g of 4VP(50)/S(50) is 120 °C (Figure 3B). Classic incompatibility results when these two copolymers are blended on a 50/50 weight basis in the absence of solvent. This claim is supported by the thermogram in Figure 3C where two distinct glass transition temperatures are detected at approximately the T_g's of the undiluted copolymers. The following ternary blends are based on a 55/45 molar ratio of 4VP(50)/S(50) and 4VP(58)/BMA(42). In these calculations of molar concentrations, the "repeat unit" molecular weight of each copolymer is based on a mole-fraction-weighted sum of the repeat unit molecular weight of each comonomer. A single glass transition process is detected by DSC at 141 °C when the molar concentration of cobalt chloride is 5% as illustrated in Figure 3F. This represents a synergistic

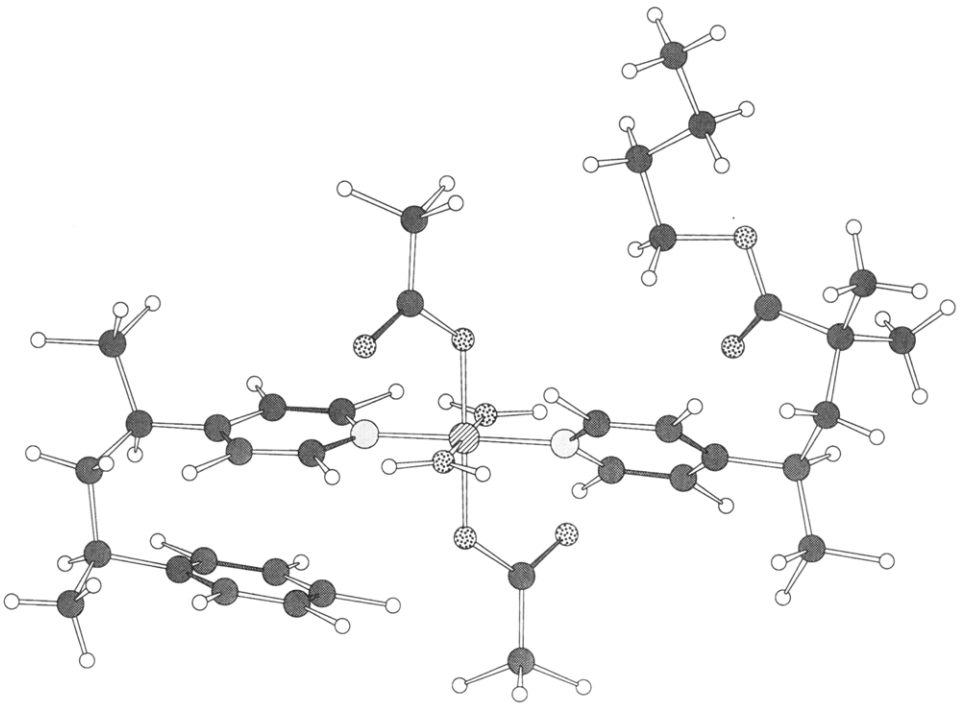

Figure 4. Molecular model that illustrates the concept of transition-metal compatibilization of two immiscible vinylpyridine copolymers. Nickel acetate tetrahydrate is the d-block metal salt that sheds two hard-base waters of hydration and coordinates to pyridine side groups in copolymers of styrene with 4-vinylpyridine and butyl methacrylate with 4-vinylpyridine.

response of 21 °C with respect to the highest T_g of the two undiluted copolymers [4VP(50)/S(50)]. At 11 mol % cobalt chloride, the DSC trace in Figure 3G reveals one T_g at 157 °C representing a synergistic increase of 37 °C. When the glass transition temperature response is detected via calorimetry, the synergistic effect correlates directly with the concentration of cobalt chloride in these ternary mixtures.

The ternary blend that contains 3 mol % nickel acetate reveals two glass transitions that are relatively weak at 85 °C and 133 °C as illustrated in Figure 3D. Incompatibility is prevalent, but the nickel salt induces a slight T_g enhancement in each separate phase. At 9 mol % nickel acetate, a single glass transition process is detected at 140 °C in Figure 3E. In light of the crystal structure of nickel acetate tetrahydrate,[8,9] a simple molecular model is depicted in Figure 4 which suggests that the nickel cation sheds two waters of hydration and coordinates to pyridine side groups on two dissimilar copolymer chains to generate a miscible ternary blend. When the ternaries contain 12, 15, and 22 mol % nickel acetate, no glass transition process is detected below 200 °C. Interestingly enough, when a single T_g is measured, it is above the 120 °C value of the random 50/50 copolymer of styrene and 4-vinylpyridine, and thermal synergy is reported relative to 120 °C. At comparable concentrations of the low-molecular-weight metal salt, the synergistic enhancement in T_g is larger for binary mixtures of nickel acetate with P4VP[1,2] relative to the ternary copolymer blends described herein. Styrene and butyl methacrylate copolymer segments are inert from the viewpoint of coordination cross-linking. Except for the ternary blend that contains 3 mol % nickel acetate, no glass transition process is measured in the vicinity of 80 °C, characteristic of the random 58/42 copolymer of 4-vinylpyridine with butyl methacrylate. The results presented in Figure 3 differ from those reported by Jiang et al.[40] who investigated the same types of copolymers but the 4-vinylpyridine content was only 12 mol % in each case. Consequently, a variety of divalent metal acetates induces *partial compatibilization* in ternary blends due to the fact that the lower T_g of 4VP(12)/BMA(88) increases and the higher T_g of the 4VP(12)/S(88) copolymer decreases.[40] No synergistic enhancement in thermal transition temperatures was reported. If all of the data on these ternary blends are self-consistent and solvent effects are minimized, then one might speculate that the 4-vinylpyridine content in the two copolymers controls the ability of d-block metal salts to induce compatibilization, coordination cross-linking, and thermal synergy.

Synergistic Thermal Response in Blends of Poly(4-vinylpyridine) with the Dimer of Dichlorotricarbonylruthenium(II). As mentioned above, the stoichiometric complex of dichlorotricarbonylruthenium(II) with P4VP, which contains a 1:1 molar ratio of ruthenium to pyridine nitrogen, reveals no glass transition process below 300 °C. At a concentration of 10 mol % ruthenium, no T_g is observed in the calorimeter trace below 300 °C, also. Furthermore, no glass transition process is observed below ≈220 °C for the complex that contains 5 mol % ruthenium. Thermal degradation of the 5 mol % ruthenium complex dominates the calorimeter trace above 220 °C. When the concentration of ruthenium in the polymeric complex is reduced significantly, glass transition temperatures are detected in the DSC thermograms as illustrated in Figure 5. The T_g-composition phase diagram for blends that contain between 0 and 3 mol % ruthenium is provided in the insert to Figure 5. A linear increase in the glass transition temperature is observed: 145 °C for undiluted P4VP, 155 °C for the 1 mol % ruthenium complex, 165 °C for the 2 mol % ruthenium complex, and 175 °C for the 3 mol % ruthenium complex. The trend in the phase diagram suggests that a percolation model[33-35] could explain coordination cross-linking with the threshold concentration of ruthenium between 3 and 5 mol %. In contrast to the hypotheses in this study, Forster and Vos[41] synthesized osmium- and ruthenium-containing metallopolymers based on poly(4-vinylpyridine) and poly(*N*-vinylimidazole) with enhanced glass transition temperatures. However, the synthetic approach relied on chemical reaction between the metal–bis(2,2′-bipyridyl) centers and

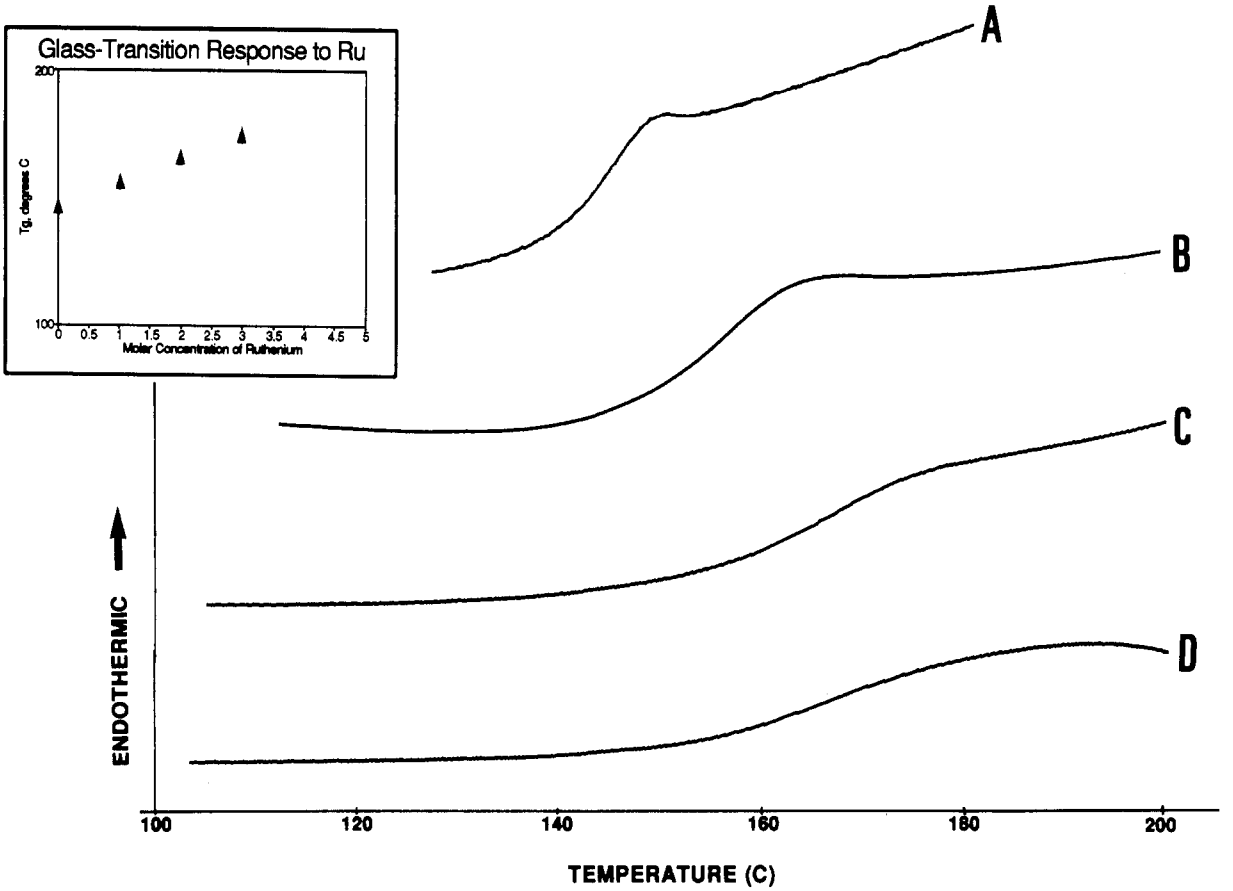

Figure 5. Differential scanning calorimetry thermograms for coordination complexes of poly(4-vinylpyridine) with the dimer of dichlorotricarbonylruthenium(II). The uppermost trace (A) represents the undiluted polymer. Thermograms B, C, and D represent binary mixtures of P4VP that contain 1, 2, and 3 mol %, respectively, of the ruthenium dimer. The glass transition temperature phase diagram is provided in the insert for low concentrations of the ruthenium salt. A percolation threshold for coordination cross-linking, as detected by calorimetry, occurs between 3 and 5 mol % dichlorotricarbonylruthenium(II).

preformed vinyl polymers without the formation of cross-links to generate soluble complexes. Calorimetric data reveal that glass transition temperatures are significantly enhanced relative to the undiluted vinyl polymers. Maximum synergy for osmium/P4VP is 109 °C, and the largest enhancement for osmium/PNVI is 96 °C.[41] No corresponding data were reported for the ruthenium-based polymers.

Infrared Study of Ruthenium Complexes with Poly(4-vinylpyridine). Infrared spectroscopy is employed in this section to provide molecular-level support for coordination interactions between poly(4-vinylpyridine) and the ruthenium dimer. Ruthenium–carbon vibrational absorptions between 450–650 cm^{-1} (Figure 6), CO stretching modes between 1900–2200 cm^{-1} (Figure 7), and carbon–nitrogen and carbon–carbon vibrational absorptions of the pyridine ring in the vicinity of 1400–1600 wavenumbers (Figure 8) suggest that the dihalogen bridge of $[Ru(CO)_3Cl_2]_2$ is cleaved in the 1:1 complex. The infrared data are consistent with electron transfer reactions due to (i) σ-bonding between the pyridine nitrogen lone pair and the appropriate molecular orbitals (e_g) of the metal center in the octahedral point group, and (ii) backbonding between the t_{2g} molecular orbitals of ruthenium and the π^* antibonding orbitals of carbon monoxide. Dichlorotricarbonylruthenium(II) crystals dispersed in KBr pellets absorb infrared radiation at 468, 480, 564, 574, and 611 wavenumbers, characteristic of metal–carbon vibrations[22,24] as illustrated in Figure 6. The analogous infrared absorptions of the P4VP–ruthenium complex that represent metal–carbon stretching modes lack the "fine structure" that is prevalent in the undiluted ruthenium

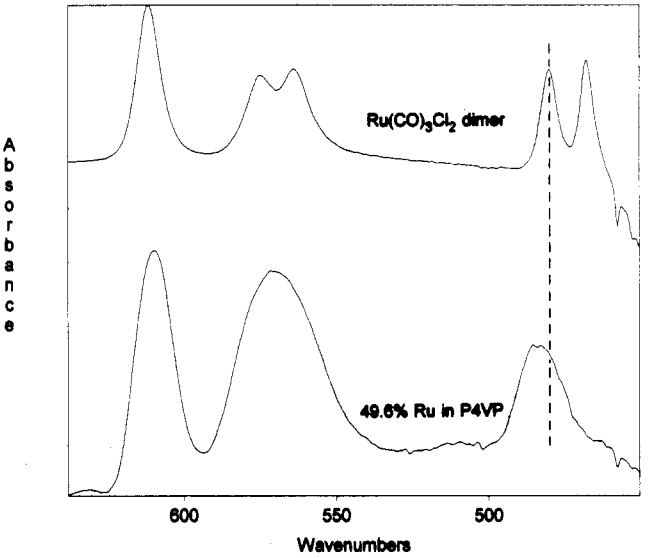

Figure 6. Fourier transform infrared spectra of the undiluted ruthenium dimer (upper spectrum) and the P4VP–ruthenium complex (lower spectrum) focusing on ruthenium–carbon vibrational absorptions between 450 and 650 wavenumbers. The stretching mode highlighted by the dashed line suggests that ruthenium–carbon bonds are strengthened slightly in the polymeric complex relative to the dimer. The spectrometer resolution is 1 wavenumber in both cases.

salt. For example, the doublet at 564 and 574 wavenumbers in the salt appears as one "averaged" broad absorption at 570 cm^{-1} in the complex with P4VP. The doublet at 468 and 480 wavenumbers in the salt is broadened and shifted to 484 cm^{-1} in the polymeric complex. This effect

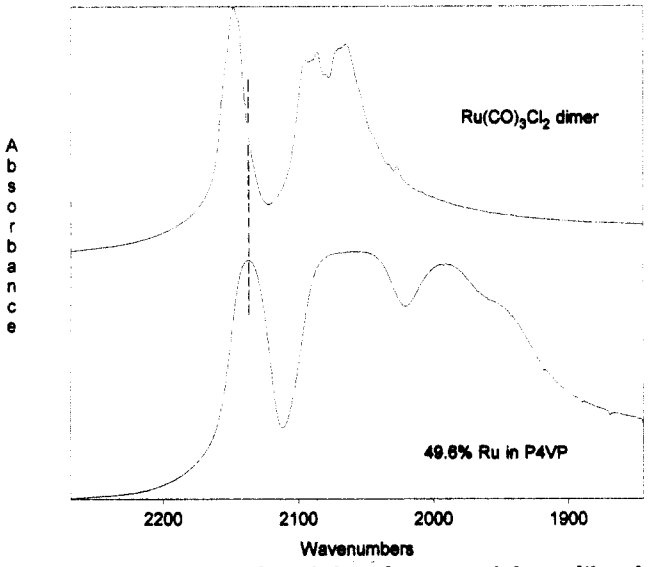

Figure 7. Fourier transform infrared spectra of the undiluted ruthenium dimer (upper spectrum) and the P4VP–ruthenium complex (lower spectrum) focusing on IR stretching modes of the carbonyl ligands between 1900 and 2200 wavenumbers. On the basis of the vibrational absorption indicated by the dashed line, CO bonds are weaker in the complex relative to the dimer. In conjunction with the broad absorption of the complex below 2000 cm^{-1} (lower spectrum) which is absent in the undiluted dimer, this result is consistent with the π-back-donation model where electron density from the metal populates the antibonding molecular orbitals of CO. The spectrometer resolution is 1 wavenumber in both cases.

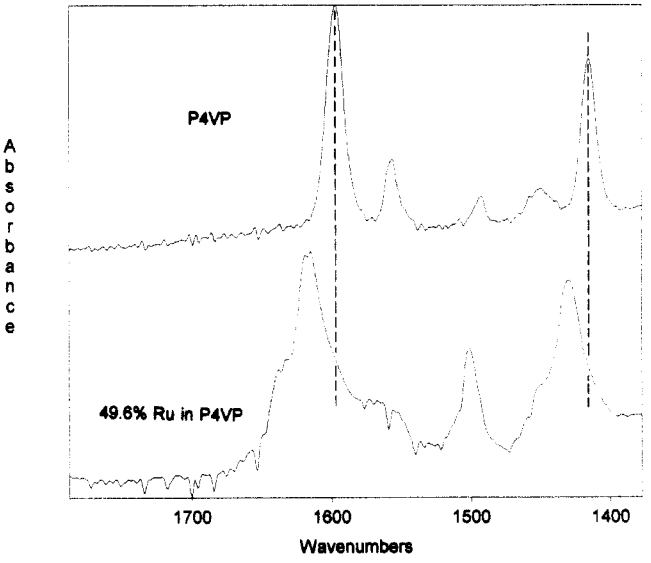

Figure 8. Fourier transform infrared spectra of undiluted poly(4-vinylpyridine) (upper spectrum) and the P4VP–ruthenium complex (lower spectrum) focusing on carbon–nitrogen and carbon–carbon vibrational absorptions of a pyridine ring which is substituted in the 4-position by the vinyl backbone of the polymer. The dashed lines identify the infrared frequencies of the strongest absorptions for the undiluted polymer in this region of the spectrum. These absorptions shift to higher energy in the polymeric ruthenium complex by 15–20 wavenumbers. The lower spectrum of the complex also reveals weak low-energy shoulders on both strong absorptions that are characteristic of pyridine side groups in the polymer which do not coordinate to ruthenium. The spectrometer resolution is 2 wavenumbers in both cases.

is highlighted by the dashed line on the right side of Figure 6. The 611 cm^{-1} signal is essentially unaffected by blending. The signal at 484 cm^{-1} (Figure 6) in the polymeric complex relative to the 468/480 cm^{-1} doublet in the ruthenium dimer suggests that ruthenium–carbonyl bonds are strengthened slightly when the dihalogen bridge of $[Ru(CO_3)Cl_2]_2$ is cleaved and a "strong-base" pyridine side group coordinates to the metal center. This conclusion is reasonable because the pyridine nitrogen lone pair occupies a ligand molecular orbital with local σ-symmetry about the metal–ligand bond axis and contributes electron density to the metal via σ-bonding. Consequently, this input of negative charge to the ruthenium cation is delocalized over the π-acceptor CO ligands via backbonding. Hence, π-bonds form between the t_{2g} orbitals of the metal and the π^* antibonding orbitals of carbon monoxide.[21] Molecular orbital theory suggests that these relatively low-lying empty π^* orbitals of CO have their largest amplitude on the carbon atom[21] which is bonded to ruthenium. In contrast, the full π-bonding orbitals of CO are primarily localized on the oxygen atom[21] and they cannot overlap the t_{2g} orbitals of the metal. Hence, the ruthenium–carbon bond is strengthened via π-bonding and the CO bond weakens because the π^* antibonding orbitals of carbon monoxide are populated via π-back-donation. Infrared evidence is available in the CO stretching region of the spectrum to support the claim that the CO bond weakens as a consequence of π-bonding. Solution-state infrared experiments identify either two or three carbonyl signals for $[Ru(CO)_3Cl_2]_2$ in hexane, benzene, carbon tetrachloride, chloroform, or methylene chloride.[22] Solid-state FTIR spectra in a KBr medium reveal multiple signals over the 1900–2200 cm^{-1} frequency range as illustrated in Figure 7. Infrared data for the CO vibrational absorptions are consistent with terminal ligands,[21] both in the crystalline dimer and in the polymeric ruthenium complex. Most notably, the CO stretch at 2148 cm^{-1} shifts 11 wavenumbers to lower energy in the P4VP–ruthenium complex, indicative of a weaker CO bond when pyridine side groups coordinate to ruthenium. This effect is highlighted by the dashed line in Figure 7. Infrared data in the CO stretching region of the spectrum also reveal a strong and rather broad absorption below 2000 wavenumbers in the polymeric complex that is absent in the undiluted dimer (Figure 7). This represents further evidence that CO bonds are weaker when a coordination complex forms between the ruthenium salt and P4VP. In summary, the infrared data in Figures 6 and 7 support the bonding model described in ref 21 when CO ligands coordinate to transition metals.

Complementary infrared signals for the aromatic in-plane carbon–nitrogen and carbon–carbon stretches of a pyridine ring that is substituted in the 4-position by the vinyl polymer backbone support the conclusion that P4VP side groups coordinate to ruthenium. In the undiluted polymer, the strongest vibrational absorptions characteristic of these stretching modes are identified at 1415 and 1597 cm^{-1} in the upper spectrum of Figure 8. These assignments are consistent with tabulated infrared data in refs 36 and 37. After complexation to the ruthenium salt, the 1597 cm^{-1} absorption in the upper spectrum of Figure 8 is broadened and shifted 18 wavenumbers to higher energy as illustrated in the lower spectrum of Figure 8. A low-wavenumber shoulder on the broad 1615 cm^{-1} absorption in the lower spectrum in the vicinity of the "free" carbon–nitrogen stretch at 1597 cm^{-1}, highlighted by the dashed line on the left side of Figure 8, suggests that all of the pyridine side groups do not participate in the coordination interaction. A similar set of observations and conclusions applies to the 1415 cm^{-1} signal in the undiluted polymer and the 1430 cm^{-1} signal in the polymeric ruthenium complex. This phenomenon is highlighted by the dashed line on the right side of Figure 8. No satisfactory molecular orbital explanation is available to account for the fact that carbon–nitrogen and

carbon–carbon stretches within the pyridine ring shift to higher energy in the polymeric ruthenium complex relative to undiluted P4VP. The infrared trends observed herein for in-plane vibrational absorptions of a substituted pyridine ring are similar to those reported by Lundberg et al.[12] for blends of zinc-neutralized sulfonated EPDM with a styrene/4-vinylpyridine copolymer. Previous studies that originated in this laboratory for zinc acetate/P4VP,[27] zinc laurate/P4VP,[27] zinc stearate/P4VP,[28] and P4VP with a zinc-neutralized copolymer of ethylene and methacrylic acid[1] also suggest that the strong infrared vibrations of the pyridine ring shift to higher energy in the coordination complex. Along similar lines, infrared spectroscopic studies of specific interactions in miscible blends of poly(hydroxymethacrylates) with poly(vinylpyridines) by Cesteros et al.[39] reveal that stretching modes of the pyridine ring in the vicinity of 1590–1600 cm^{-1} shift to higher energy when hydrogen bonds are operative. The explanation of the frequency shift is rather qualitative, mentioning altered electronic distributions in the ring and the formation of stronger bonds.

Carbon-13 Solid State NMR Spectroscopy of P4VP–Ruthenium Complexes. d-Block metals must have a vanishing electron magnetic moment to obtain high-resolution ^{13}C NMR signals of directly-bound ligands. In this respect, the NMR experiments described herein focus on diamagnetic d^6 octahedral complexes. The dimer of dichlorotricarbonylruthenium(II) is attractive because this d^6 complex is diamagnetic in an octahedral environment. The carbonyl ligands contribute to strong-field zero-electron-spin behavior[21] and eliminate spectral broadening effects due to potential paramagnetic metal centers. Two magnetically active quadrupolar isotopes of ruthenium exist, ^{99}Ru and ^{101}Ru, with natural isotopic abundances of approximately 13 and 17%, respectively. Hence, it is feasible to generate "high-resolution" carbon-13 solid-state NMR spectra of the carbonyl ligands in the coordination sphere of ruthenium. Carbonyl ^{13}C signals in the undiluted d-block dimer, $[Ru(CO)_3Cl_2]_2$, are accessible via the "Bloch decay" pulse sequence with magic-angle spinning. In this case, ^1H–^{13}C cross polarization is not feasible because the molecule contains no protons. Along similar lines, Shoemaker and Apple[29] successfully observed high-resolution ^{13}C solid-state NMR signals for carbon monoxide adsorbed on ruthenium-exchanged zeolite catalysts using the Carr–Purcell spin-echo pulse sequence.[30] Standard cross-polarization/magic-angle-spinning/dipolar-decoupled ^{13}C NMR experiments should generate signals for the ruthenium carbonyl salt when it forms a coordination complex with poly(4-vinylpyridine). In this case, the well-established cross-polarization mechanism of heteronuclear spin diffusion between the proton spin manifold of the polymer and the carbonyl carbons of the d-block salt provides a tool to evaluate mixing characteristics at the molecular level.[31,32]

The application of NMR spectroscopy described herein is unusual due to (i) the choice of the d-block metal salt and (ii) details associated with the ^1H–^{13}C cross-polarization process for solids. The overall objective is to identify poly(4-vinylpyridine) and the ruthenium salt as nearest neighbors in the blend that contains stoichiometric proportions of ruthenium to pyridine. Molecular-level information of this nature, in conjunction with the FTIR data described above, supports the hypothesis of a polymeric coordination complex that exhibits a glass transition temperature in excess of 300 °C. The experiment is designed for rigid solids with strong dipolar couplings between ^1H and ^{13}C nuclides. Proton-enhanced

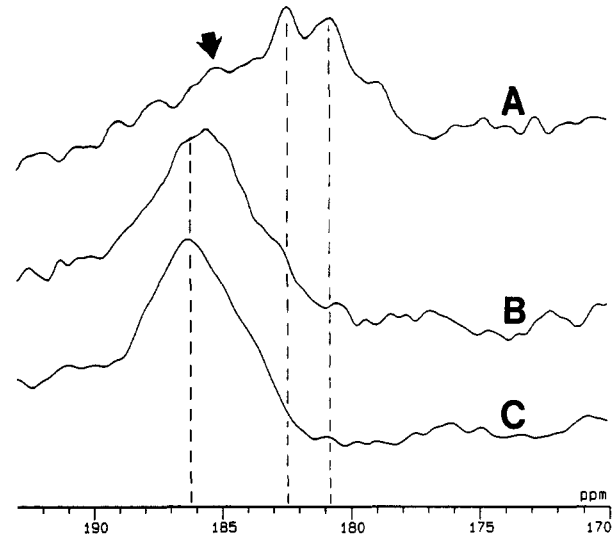

Figure 9. High-resolution carbon-13 solid-state NMR spectra of the carbonyl ligands in the undiluted ruthenium dimer (spectrum A) and the P4VP–ruthenium complex (spectra B and C). Spectrum A was obtained via the Bloch decay pulse sequence with a repetition delay of 60 s and 50 Hz of line broadening. Spectrum B was obtained for the complex that contains 1 mol of ruthenium per 1 mol of pyridine side groups in the polymer. This spectrum was generated via 2 ms of ^1H–^{13}C cross polarization thermal contact and 50 Hz of line broadening, suggesting that the two dissimilar molecules are in close proximity. Spectrum C represents the same polymeric ruthenium complex, but the Bloch decay pulse sequence was used with a repetition delay of 30 s and 50 Hz of line broadening. The dashed lines highlight the strongest carbonyl ^{13}C resonances in the undiluted dimer at 181 and 182.5 ppm and in the polymeric complex at 186 ppm. The arrow in spectrum A identifies a weaker resonance of the crystalline dimer at 185.5 ppm that exhibits a distinct spinning sideband at 251.5 ppm in Figure 11.

carbon-13 NMR spectra of solids are generated via heteronuclear spin diffusion between dipolar-coupled nuclei that typically reside within the same molecule. Protons are polarized and spin-locked in the rotating reference frame such that the ^1H manifold is highly ordered and characterized by a spin temperature approximately 3 orders of magnitude smaller than the equilibrium spin temperature of the abundant protons in the static magnetic field. On the other hand, the carbon-13 spin system is extremely warm by virtue of the fact that ^{13}C polarization is nonexistent in the rotating reference frame before spin diffusion occurs. The large spin-temperature difference between ^1H and ^{13}C magnetic moments provides the driving force, and heteronuclear dipolar couplings provide the mechanism for polarization transfer from protons to carbons in the rotating reference frame. Since these mutual spin–spin flips are designed to be energy-conserving, the overall process occurs typically on the short millisecond time scale if (i) the two nuclei are in close proximity, and (ii) the static contribution to the spectral density function that characterizes micro-Brownian motion is large enough, as it is in rigid solids. When one considers the undiluted ruthenium dimer, it is obvious that the cross-polarization process is not feasible because the molecule lacks protons. In this respect, the one-pulse Bloch-decay sequence using a repetition delay of 60 s is employed to obtain the ^{13}C spectrum of the carbonyl ligands as illustrated in Figure 9A. The resonance envelope reveals that there are at least two crystallographically inequivalent CO groups that give rise to ^{13}C chemical shifts at 181 and 182.5 ppm indicated by the two dashed lines at lower chemical shift in Figure 9A. The crystal structure

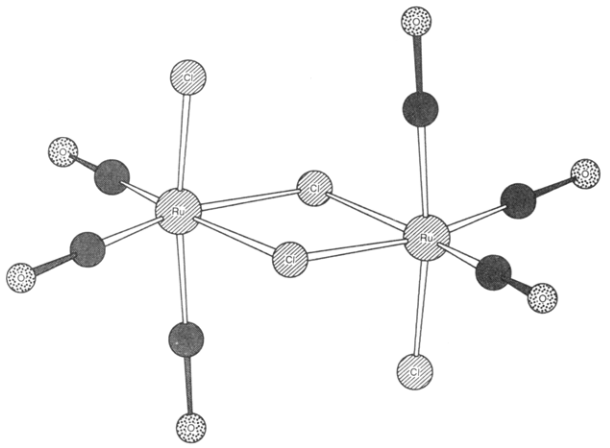

Figure 10. Molecular model illustrating the crystal structure of the dimer of dichlorotricarbonylruthenium(II) with a dihalogen bridge between the two metal centers in a pseudooctahedral configuration. Adopted from refs 10 and 22.

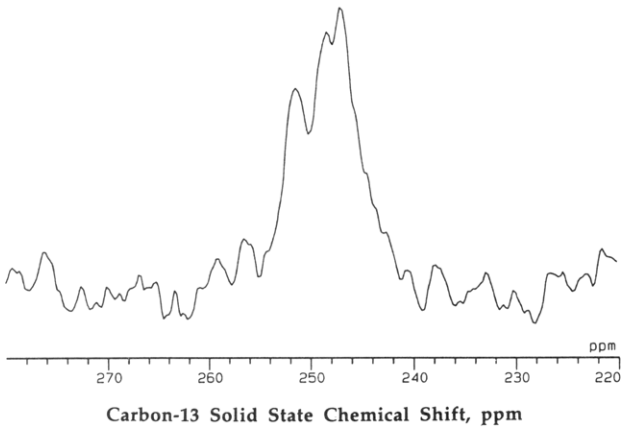

Figure 11. High-resolution carbon-13 solid-state NMR spectrum of the carbonyl ligands in the undiluted ruthenium dimer via the Bloch decay sequence with a repetition delay of 60 s and 50 Hz of line broadening. Magic-angle spinning was performed at a nominal rate of 5 kHz. This spectrum in the vicinity of 250 ppm focuses on the first spinning sideband pattern at higher chemical shift relative to the isotropic signals, illustrated in spectrum 9A, between 180 and 190 ppm. The weaker signal at 251.5 ppm represents the first spinning sideband for the parent signal indicated by the arrow in spectrum 9A.

of $[Ru(CO)_3Cl_2]_2$ illustrated in Figure 10 indicates that there are four in-plane (equatorial) and two out-of-plane (apical) carbonyl ligands relative to the orientation of the dihalogen bridge.[10,22] The chemical shift anisotropy of the carbonyl ^{13}C shielding tensor is large enough to generate a spinning sideband pattern that reveals more fine structure than the isotropic signal. At a rotor speed of 5 kHz, the first spinning sideband envelope in the vicinity of 250 ppm is more intense than the isotropic signal, and its fine structure is illustrated in Figure 11. When one considers the signal-to-noise ratio, it is only reasonable to identify two absorptions in the first spinning sideband pattern to the left of the isotropic resonance envelope on the chemical shift axis. The crystal structure of $[Ru(CO)_3Cl_2]_2$ illustrated in Figure 10 suggests a tentative assignment of the ^{13}C NMR sideband pattern in Figure 11 as follows. Four equatorial carbonyl ligands produce the stronger absorption at 247–248.5 ppm in Figure 11 on the basis of the parent signals at 181 and 182.5 ppm in Figure 9A. Two apical carbonyls generate the weaker absorption at 251.5 ppm in Figure 11 for the isotropic signal that is identified by the arrow at 185.5 ppm in Figure 9A. Each isotropic resonance is separated from its first spinning sideband by 66 ppm which corresponds to an actual rotor speed of 4982 Hz. This compares well with the nominal spinning speed of 5 kHz.

When one considers the ruthenium coordination complex with P4VP, the rigidity of the blend is unquestioned from the viewpoint of efficient intermolecular polarization transfer. The proximity of ^1H nuclei in the polymer to ^{13}C nuclei in the d-block metal salt can be addressed qualitatively via magnetization transport. The proton-enhanced ^{13}C NMR spectrum of the carbonyl ligands in the polymeric ruthenium complex is illustrated in Figure 9B at a cross-polarization contact time of 2 ms. It is obvious that the ruthenium salt and P4VP are nearest neighbors, which facilitates heteronuclear spin diffusion and the appearance of carbonyl ^{13}C signals in the middle spectrum of Figure 9. Two milliseconds of cross polarization thermal contact is a typical duration for heteronuclear spin diffusion when proton and carbon nuclei reside within the same molecule. This suggests that dipolar distances between P4VP protons and carbonyl ^{13}C sites in the ruthenium salt are comparable to intramolecular distances. When spectrum 9B is compared to spectrum 9A, the following observation is readily apparent. The isotropic chemical shift of the carbonyl signal in the polymeric ruthenium complex shifts downfield to 186 ppm relative to the ^{13}C NMR absorptions of the undiluted crystalline dimer illustrated in spectrum 9A. This chemical shift perturbation of 4–5 ppm for the carbonyl ^{13}C signal is reasonable if (i) the dihalogen bridge of $[Ru(CO)_3Cl_2]_2$ is cleaved during the blending process and (ii) one or two pyridine side groups in P4VP coordinate to the metal center in an amorphous complex. A second explanation of the spectral changes in Figure 9 focuses on the fact that the weak signal at 185.5 ppm in the undiluted ruthenium dimer (identified by the arrow in spectrum 9A) persists after coordination to the polymer, whereas the stronger signals at 181 ppm and 182.5 ppm in the undiluted salt are nonexisting after blending. Confirmation of this second explanation should be based on the fate of the equatorial and apical carbonyl ligands in Figure 10 after the dihalogen bridge in the undiluted ruthenium dimer is cleaved by P4VP upon blending. The lowermost spectrum of the polymeric ruthenium complex in Figure 9C was obtained using the one-pulse Bloch decay sequence with a repetition delay of 30 s. In this case, carbonyl ligands in the coordination sphere of ruthenium are polarized and detected in the NMR experiment without the requirement that P4VP protons be in close proximity. Hence, spectrum 9C does not independently support the hypothesis that the ruthenium salt and P4VP are nearest neighbors. However, the lowermost spectrum in Figure 9C is extremely similar in appearance to spectrum 9B, and this middle spectrum in Figure 9B argues strongly that a polymeric complex forms between P4VP and dichlorotricarbonylruthenium(II).

Conclusions

Low-molecular-weight d-block transition metal salts containing cobalt, nickel, and ruthenium were blended separately with 4-vinylpyridine homopolymers and copolymers to generate mixtures that exhibit enhanced glass transition temperatures. In each case where T_g can be measured by differential scanning calorimetry, thermal synergy is reported relative to the highest T_g of the pure-component polymers. Ternary blends were investigated where the cobalt or nickel salt functions as a transition-metal compatibilizer for two immiscible copolymers that contain 4-vinylpyridine repeat units in the main chain. A single tetrahedral cobalt or octahedral nickel center must coordinate to a pyridine nitrogen lone pair in each

copolymer to generate miscible ternary blends. Spectroscopic studies were performed on binary mixtures of poly(4-vinylpyridine) with the dimer of dichlorotricarbonylruthenium(II) to obtain molecular-level support for the proposed polymeric coordination complexes that are completely amorphous. Infrared spectroscopy suggests that ruthenium-carbon bonds are strengthened slightly in the polymeric complex relative to the undiluted crystalline dimer. This effect is rationalized by π-backbonding between the metal center and the carbonyl ligands when strong σ-donors like pyridine cleave the dihalogen bridge and coordinate to ruthenium. CO infrared stretching frequencies are subsequently weaker because π-bonds form between the t_{2g} orbitals of ruthenium and the π^* antibonding orbitals of carbon monoxide. High-resolution solid-state carbon-13 NMR studies are rather unique in this application because one can measure heteronuclear spin diffusion between the protons in the polymer and the carbonyl carbons of the ruthenium salt during the cross-polarization segment of the rf pulse sequence. Since intermolecular polarization transfer occurs within 2 ms, the NMR results support the hypothesis that the two dissimilar molecules are nearest neighbors. The ^{13}C isotropic chemical shift of the carbonyl carbon in the ruthenium salt is sensitive to the other ligands in the coordination sphere of the metal. Hence, the resonance envelope is observed 4–5 ppm downfield in the polymeric complex relative to the undiluted dimer. This chemical shift perturbation is reasonable if the pyridine side group in P4VP cleaves the dihalogen bridge of $[Ru(CO)_3Cl_2]_2$ and either one or two pyridine nitrogen lone pairs form σ-bonds with ruthenium. This hypothesis is also reasonable because reactions of this nature have been reported in the organometallic literature for low-molecular-weight analogs of the polymeric complexes described in this study.

Acknowledgment. The research described herein was supported by the National Science Foundation's Division of Materials Research (Polymer program) through Grant No. DMR-9214022, the donors of the Petroleum Research Fund, administered by the American Chemical Society, and Asahi Chemical Industry in Okayama, Japan. The carbon-13 solid-state NMR spectra were obtained in collaboration with Dr. James S. Frye at Otsuka Electronics Inc., Fort Collins, CO. Eiji Ueda acknowledges Asahi Chemical Industry for research support as a visiting scientist at Colorado State University.

References and Notes

(1) Belfiore, L. A.; Graham, H.; Ueda, E.; Wang, Y. *Polym. Int.* **1992**, *28*, 81.
(2) Belfiore, L. A.; Graham, H.; Ueda, E. *Macromolecules* **1992**, *25*, 2935.
(3) Khandwe, M.; Bajpai, A.; Bajpai, U. D. N. *Macromolecules* **1991**, *24*, 5203.
(4) Belfiore, L. A. Direct Evidence for Transition-Metal Coordination in Polymer Blends. *Preprints of the Second Pacific Polymer Conference*, 1991, Vol. 2, p 115.
(5) Belfiore, L. A. *Polym. Prepr.* **1992**, *33* (1), 925.
(6) *Cobalt: Its chemistry, metallurgy, and uses*; Young, R. S., Ed.; Reinhold Publishing Co.: New York, 1960; p 76.
(7) Mizuno, J.; Ukei, K.; Sugawara, T. The crystal structure of $CoCl_2$-$6H_2O$. *J. Phys. Soc. Jpn.* **1959**, *14*, 383.
(8) VanNiekerk, J. N.; Schoening, F. R. L. *Acta Crystallogr.* **1953**, *6*, 609.
(9) Downie, T. C.; Harrison, W.; Raper, E. S.; Hepworth, M. A. *Acta Crystallogr.* **1971**, *B27*, 706.
(10) Merlino, S.; Montagnoli, G. *Atti Soc. Toscana Sci. Nat. Pisa, Mem., Ser. A* **1970**, *76*, 335.
(11) Agnew, N. H. *J. Polym. Sci., Polym. Chem. Ed.* **1976**, *14*, 2819.
(12) Peiffer, D. G.; Duvdevani, I.; Agarwal, P. K.; Lundberg, R. D. *J. Polym. Sci., Polym. Lett. Ed.* **1986**, *24*, 581.
(13) Allan, J. R.; Carson, B. R.; Turvey, K.; Birnie, J.; Gerrard, D. L. *Eur. Polym. J.* **1991**, *27* (7), 665.
(14) Allan, J. R.; Carson, B. R.; Turvey, K.; Birnie, J.; Gerrard, D. L. *Thermochim. Acta* **1991**, *180*, 39.
(15) Allan, J. R.; Carson, B. R.; Paton, A. D.; Turvey, K.; Birnie, J.; Gerrard, D. L. *Plast. Rubber Compos. Process. Appl.* **1991**, *16*, 79.
(16) Cotton, F. A.; Wilkinson, G. *Advanced Inorganic Chemistry*, 3rd ed.; Wiley-Interscience: New York, 1972; Chapter 25, p 897.
(17) Admiraal, L. J.; Gafner, G. The crystal and molecular structure of dichlorobis(4-vinylpyridine)cobalt(II). *Chem. Commun.* **1968**, p 1221.
(18) Agnew, N. H.; Larkworthy, L. F. Cobalt(II) complexes of 2- and 4-vinylpyridines. *J. Chem. Soc.* **1965**, 4669.
(19) Gill, N. S.; Nyholm, R. S.; Barclay, G. A.; Christie, T. I.; Pauling, P. J. *J. Inorg. Nucl. Chem.* **1961**, *18*, 88.
(20) Pearson, R. G. In *Survey of Progress in Chemistry-Volume 6*; Scott, A., Ed.; Academic Press: New York, 1969; Chapter 1.
(21) Shriver, D. F.; Atkins, P. W.; Langford, C. H. *Inorganic Chemistry*; W. H. Freeman: New York, 1990.
(22) Benedetti, E.; Braca, G.; Sbrana, G.; Salvetti, F.; Grassi, B. *J. Organomet. Chem.* **1972**, *37*, 361.
(23) Stephenson, T. A.; Wilkinson, G. *J. Inorg. Nucl. Chem.* **1966**, *28*, 945.
(24) Cleare, M. J.; Griffith, W. P. Halogeno-carbonyl complexes of the platinum metals, and their vibrational spectra. *J. Chem. Soc.* **1969**, *A*, 372.
(25) Figgis, B. *An Introduction to Ligand Fields*; Wiley: New York, 1966; pp 36–38, 236, 237, 244, and Chapter 8.
(26) March, J. *Advanced Organic Chemistry*, 3rd ed.; Wiley: New York, 1985.
(27) Belfiore, L. A.; Pires, A. T. N.; Wang, Y.; Graham, H.; Ueda, E. *Macromolecules* **1992**, *25*, 1411.
(28) Wang, Y. Metal-ligand coordination in multicomponent polymer blends. M.S. Thesis at Colorado State University, p 56 (1991).
(29) Shoemaker, R. K.; Apple, T. M. *J. Phys. Chem.* **1985**, *89*, 3185.
(30) Slichter, C. P. *Principles of Magnetic Resonance*; Springer-Verlag: Heidelberg, 1978; Chapter 8, pp 252–3.
(31) Schaefer, J.; Stejskal, E. O.; Sefcik, M. D.; McKay, R. A. *Macromolecules* **1981**, *14*, 188, 275.
(32) Belfiore, L. A. *Polymer* **1986**, *27*, 80.
(33) Stauffer, D. *Introduction to percolation theory*; Taylor and Francis: Philadelphia, 1985.
(34) Daoud, M.; Lapp, A. *J. Phys. Condens. Matter* **1990**, *2*, 4021.
(35) Flory, P. J. *J. Am. Chem. Soc.* **1941**, *63*, 3091.
(36) Colthup, N. B.; Daly, L. H.; Wiberley, S. E. *Introduction to infrared and Raman spectroscopy*, 2nd ed.; Academic Press: New York, 1975; p 272.
(37) Smith, A. L. Applied infrared spectroscopy—fundamentals, techniques, and analytical problem solving. *Chemical Analysis*; Wiley: New York, 1979; Vol. 54, p 298.
(38) Shibayama, M.; Adachi, M.; Ikkai, F.; Kurokawa, H.; Sakurai, S.; Nomura, S. *Macromolecules* **1993**, *26*, 623.
(39) Cesteros, L. C.; Meaurio, E.; Katime, I. *Macromolecules* **1993**, *26*, 2323.
(40) Jiang, M.; Zhou, C.; Zhang, Z. *Polym. Bull.* **1993**, *30*, 455.
(41) Forster, R. J.; Vos, J. G. *Macromolecules* **1990**, *23*, 4372.